Investigation of Low-Frequency Noise of Horizontal Axis Wind Turbines by a Hybrid Approach

A. Bozorgi[1*]

Department of Mechanical Engineering, Arak University of Technology, Daneshgah Street, Arak, Iran.

Abstract
Noise pollution is known as the biggest environmental problem of the horizontal axis wind turbines. The main part of the noise is in the range of Low-Frequency Noise (LFN), since wind turbines rotate slowly. Several studies have shown that LFN could have adverse effects on the human health. In this work, LFN generated by the NREL VI wind turbine in wind speeds of 13 m/s is calculated using a hybrid approach. In this approach, the noise sources are defined on a data surface (DS), and then the noise propagating form DS is calculated. The results obtained show that a DS obtained by scaling the blade span with a size factor of 5 is appropriate for surrounding all the main sources in this problem. It means that in addition to the sources located on the blade surface, a significant part of the steady sources generating LFN is far from the blades. On the other hand, the results obtained show that the tip vortices have no significant effect on LFN.

Keywords: *Noise pollution, Human health, NREL VI.*

1. Introduction

The use of wind turbines has grown rapidly in the recent years in order to reduce the share of fossil fuels in global electricity production, and also to help provide energy security. According to the Renewables 2020 Global Status Report [1], the total capacity of wind power in the world has reached 743 GW in 2020 with 93 GW of new installations (more than 12.5% of the total capacity) that is a record-breaking. It is expected that this growth will continue in the future, and the use of wind turbines will become more widespread in the world. However, wind turbines have several environmental problems, and noise pollution, especially Low-Frequency Noise (LFN), is the most important of them.

The range of human hearing is defined for the frequencies between 20 Hz and 20 kHz, and the frequencies below this range are called infra-sound. Since the wind turbines usually rotate slowly, the main part of their noise is LFN, and is in the range of infra-sound. Several studies have introduced the LFN of wind turbines as a harmful factor on the human health that could lead to illnesses such as dizziness, vertigo, and tinnitus [2-7].

In the present work, LFN generated from the NREL VI tow-blade wind turbine with a rotational speed of 72 rpm and the wind speed of 13 m/s is calculated by a hybrid approach. In this approach, which is widely used in the wind turbine problems [8-10], the flow is simulated with high accuracy in near-field using Computational Fluid Dynamics (CFD) in order to identify the LFN sources on a DS, and in next step, the Fowcs-Williams and Hawkings (FW-H) equation [11] is applied for calculating the LFN that propagates from DS. The flow simulation has been carried out by Bozorgi *et al*. [12], and the CFD results have been validated by an experiment [13]. Here, the CFD results are used for identifying the LFN sources.

The position of DS has a significant effect on the noise calculation. If DS is defined near the blades, a part of noise sources is not surrounded by DS. On the other hand, by moving away from the blades, the increase in the mesh size reduces the accuracy of the CFD results, and consequently, reduces the accuracy of the noise source calculation. It should be noted that by moving away from the blades, the noise sources are weakened. Overall, a balance must be struck between the surrounding significant noise sources by a DS and the accuracy of noise source calculation.

The aim of this work is to investigate which steady noise sources have a significant effect on

generating LFN in this problem, and also where DS should be defined in order to surround all the significant LFN sources.

2. Noise source classification

Based on the source of generation, the noise of the horizontal axis wind turbines is classified into the mechanical and aerodynamic noises. The mechanical noise can be effectively eliminated but the aerodynamic noise is still a main problem of these turbines. According to the Wagner classification [14], which is known as a routine classification for the noise of horizontal axis wind turbines, the aerodynamic noise is divided into three categories: LFN, inflow turbulence noise, and airfoil self-noise. In this classification, LFN is due to the steady thickness noise (STN) and steady loading noise (SLN), which are located on the blade surface, and also due to the unsteady loading noise generated from the interaction of flow and tower. The latter is only significant for the downwind configurations. Therefore, according to this classification, significant sources generating LFN are located on the blade surface for the horizontal axis wind turbines with an upwind configuration. However, the results obtained by Bozorgi and Ghorbaniasl [15] show that the steady sources located far from the blades also have a significant effect on the LFN generation.

3. FW-H equation

The FW-H equation [11], as a re-arrangement of the Navier-Stokes equations, is widely used for the prediction of the noise generated by the moving bodies. By considering the free stream velocity U_∞, the generalized FW-H equation [16] is given by:

$$\left\{ \frac{1}{c_0^2} \frac{D^2}{Dt^2} - \frac{\partial^2}{\partial x_i^2} \right\} \left[p'(\mathbf{x},t) H(f) \right] =$$
$$\frac{\partial}{\partial t} \left[Q\delta(f) \right] - \frac{\partial}{\partial x_i} \left[F_i \delta(f) \right] + \frac{\partial^2}{\partial x_i \partial x_j} \left[T_{ij} H(f) \right] \quad (1)$$

Where:

$$\frac{D}{Dt} = \frac{\partial}{\partial t} + U_{\infty i} \frac{\partial}{\partial x_i} \quad (2)$$

And:

$$F_i = L_i - U_{\infty i} Q$$
$$Q = \rho(u_n - v_n) + \rho_0 v_n$$
$$L_i = \rho(u_i - U_{\infty i})(u_n - v_n) + P_{ij} n_j \quad (3)$$
$$T_{ij} = \rho(u_i - U_{\infty i})(u_j - U_{\infty j})$$
$$+ \left(p - p_0 - c_0^2 (\rho - \rho_0) \right) \delta_{ij} - \sigma_{ij}$$

In (1) to (3), c_0 is the speed of sound, Q shows the monopole sources, the L_i dipole sources, and the T_{ij} quadruple sources. The monopole and dipole sources are calculated on a DS where $f(x,t) = 0$ such that $f < 0$ is inside DS and $f > 0$ is outside DS (Figure 1). ρ is the density, and u_n and v_n are the normal components of the flow velocity and DS velocity, respectively. P_{ij} is the compressive stress tensor, and n_j is the unit normal vector of DS. Mean quantities are represented by the subscript 0, while a prime denotes a perturbation from the mean. By defining a DS on the body surface, the Q and L_i terms correspond to the thickness and loading sources, respectively. This DS is called the solid DS but DSs defined far from the body surface are called the permeable DSs.

Ghorbaniasl and Lacor [16] have developed formulations that can be interpreted as the formulations 1 and 1A for the generalized FW-H equation. These formulations have the advantage of considering the effect of mean flow on the noise calculation. Here, the formulation 1A [16] is used for the LFN calculation.
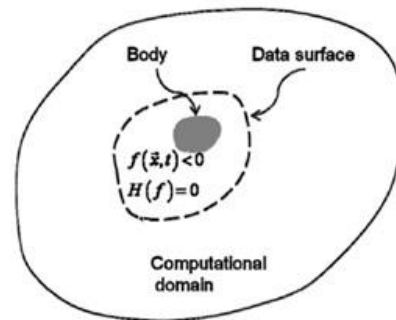

Figure 1. Description of DS position [16].

4. Results and discussion

In order to calculate LFN in far-field, several DSs are defined around the blade by scaling the blade span (Table 1).

According to the IEC 61400-11 standard, the microphone is located in the downstream at:

$$R_H = H + D/2; \; R_V = H \quad (4)$$

where R_H and R_v are the horizontal and vertical distances from the rotor center, respectively; D is the turbine diameter, and H is the hub height.

Table 1. DS Properties.

DS	Span scale factor	DS Type
DS 1	1	Impermeable
DS 1.2	1.2	Permeable
DS 1.5	1.5	Permeable
DS 2	2	Permeable
DS 3	3	Permeable
DS 4	4	Permeable
DS 5	5	Permeable

Using (4), the microphone position is at R = 21 m and θ = –55° (R and θ are shown in figure 2) for the NREL VI turbine. Here, LFN is calculated in the microphone position and also in the other positions with R = 21 m and –75° ≤ θ ≤ + 75°. Outside of this θ range, LFN is very weak such that in the rotation axis (where θ = −90° and +90°), the Overall Sound Pressure Level (OASPL) goes to −∞ dB. It can be shown by the formulation 1A [16] that LFN is generated by the steady noise source only when the distance between the source and the observer changes. However, on the rotation axis, this distance is unchanged when the blades rotate. Therefore, the LFN on the axis is zero (or −∞ in the logarithmic scale).
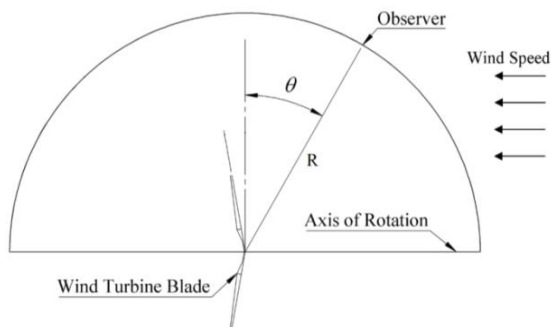

Figure 2. Position of the observers [12].

Investigation of the OASPL calculated in all the observer positions (Figure 3) shows that the results of the solid and permeable DSs are close together in downstream (θ < 0) but there is a considerable difference between the results in the upstream (θ > 0). For example, the OASPL difference at θ = 15° is about 5 dB. Here, the proper position of DS is defined where the difference between the LFN calculated from two consecutive DSs reaches less than 0.5 dB (as the convergence criterion) in all the observer positions.

It is observed that the DS 5 satisfies the convergence criterion, which means that a wide domain around the blade must be simulated with a high accuracy to have an agreeable LFN calculation. Overall, it can be concluded that in addition to the STN and SLN sources defined on the blade surface, the flow around the blade has an important effect on the LFN generation.

Moreover, it is observed that the maximum LFN is located in downstream at θ = –30°, which is far from the microphone position introduced by the IEC 61-400 standard (θ = –55°). In –45° ≤ θ ≤ 0°, LFN is more than LFN of the microphone position.

As shown in table 1, only the span expansion is performed for defining DSs. For investigating the effect of tip vortices located out of the rotor diameter, DS 3 is radially expanded using several scale factors up to 1.05 (the blade radius is equal to 5.029 m that with the scale factor of 1.05 reaches 5.55 m). The results obtained (figure 4) show that the effect of the tip vortices on LFN is ignorable. Therefore, it can be concluded that the tip vortices have no significant effect on LFN.

In figure 5, the directivity pattern obtained from the Q and L_i terms are shown for DS 1 (blade surface) and DS 5, satisfying the convergence criterion. The results obtained show that LFN of the Q and L_i terms propagating form DS 5 is considerably higher than DS 1. The change in LFN generated by the Q term is more than 10 dB in some observer positions, while the change for the L_i term is less than 3 dB in all the observer positions. It means that the flow domain has more effects on LFN of the Q term in comparison with the L_i term.
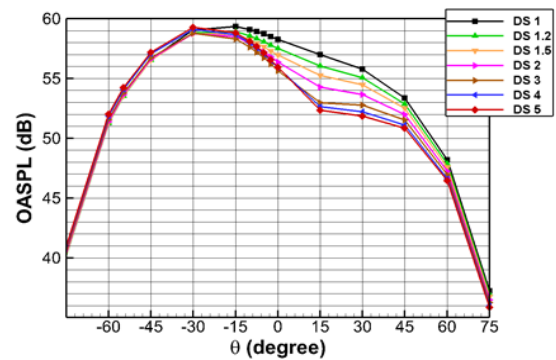

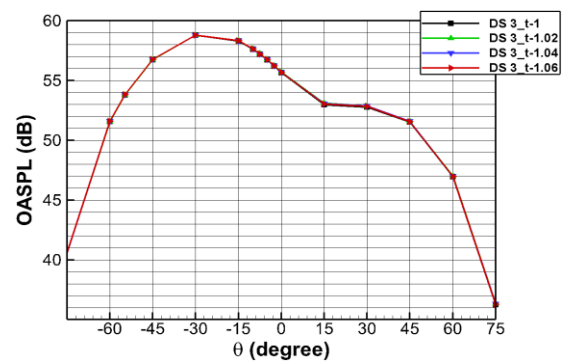**Figure 3. Effect of DS position on LFN.**

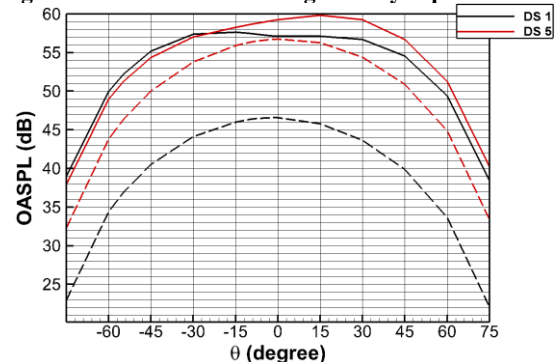**Figure 4. LFN calculated using radially expanded DS 3.**

Figure 5. Directivity for the Q (-----) and L_i (———) terms.

A more detailed investigation on the results obtained using DS 5 (Figure 5) shows that the numerical sum of LFN of the Q and L_i terms in upstream ($\theta > 0$) is more than the numerical sum in downstream ($\theta < 0$). On the other hand, the results of Figure 3 show that LFN in upstream is less than it in downstream. This apparent mismatch is due to the phase difference that there is between LFN of the Q and L_i terms. For example, the results of LFN calculated using DS 5 are shown in Figure 6 for two observer positions. An observer is located in upstream ($\theta = +30^o$), and another in downstream ($\theta = -30^o$). It is observed that LFN of the L_i term at $\theta = +30^o$ is more than it at $\theta = -30^o$ but since the Q and L_i terms weaken each other at $\theta = +30^o$, LFN received to this observer position is lower than LFN received to another observer position with $\theta = -30^o$.
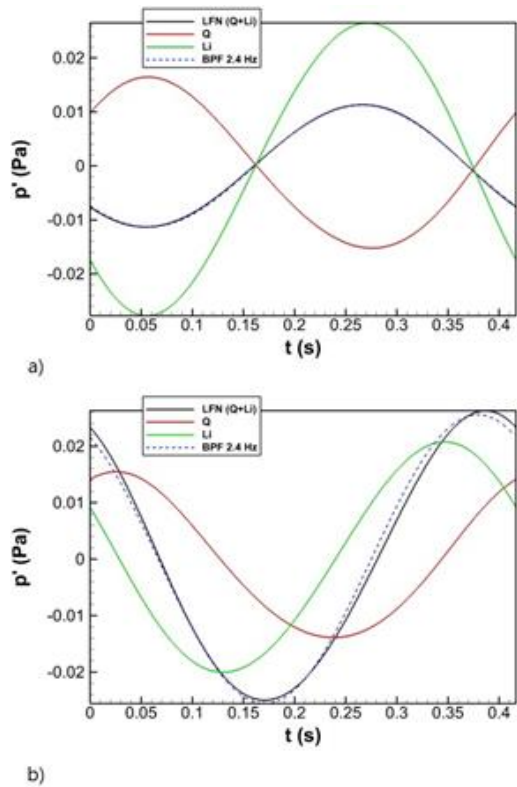

Figure 6. Pressure fluctuations received to the observers.

a) upstream $\theta = +30^o$. b) downstream $\theta = -30^o$.

Moreover, as shown in figure 6, LFN has a small deviation from a tonal noise with Blade Passing Frequency (BPF = 2.4 Hz). This small deviation is due to the deviation of the source-observer distance from a sinusoidal time function.

For more investigation, the Fast Fourier Transform (FFT) is performed on a period of the LFN received by the observers located at $\theta = +30^o$ and -30°, and the Sound Pressure Level (SPL) is calculated for the frequencies up to 50 Hz (Figure 7). The results obtained show that SPL of BPF is considerably higher than SPL of the second BPF

(more than 10 dB). Moreover, it is observed that SPL in higher frequencies is very low, and can practically be ignored in the both observer positions.
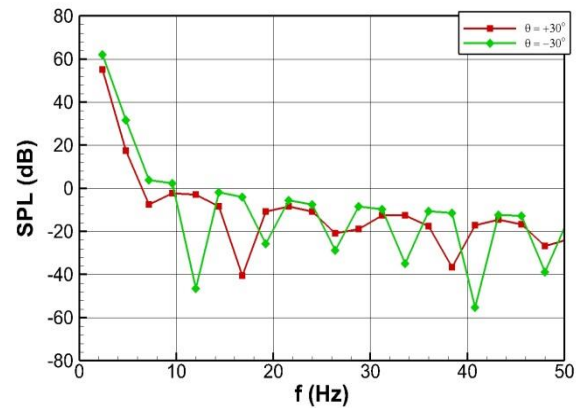

Figure 7. SPL for $\theta = +30^o$ and $\theta = -30^o$.

5. Conclusions

In the present work, LFN generated by the NREL VI wind turbine with a 72 rpm rotational speed and a 13 m/s wind speed was investigated by a hybrid approach. In this approach, the CFD results of flow simulation in near-field were used in order to calculate the LFN sources on a DS to calculate LFN in far-field. Here, the noise sources were defined on several DSs, and LFN was calculated in different observer positions.

The results of the present work show that in addition to the STN and SLN sources, the steady sources located on flow field significantly participate in the LFN generation. The results obtained show that DS 5 surrounds all the important steady sources in this test case. Therefore, a permeable DS located far from the blade must be used for the LFN calculation. On the other hand, it was observed that the tip vortices had no considerable effect on LFN.

Moreover, the maximum LFN is located in downstream since the monopole and dipole terms amplify each other in downstream, while they weaken each other in upstream. However, the position of the microphone obtained using the IEC 61400-11 standard is far from the maximum LFN of this test case.

6. Acknowledgment

7. References

[1] REN21. (2021). Renewables 2020 Global Status Report. Paris, REN21 Secretariat.

[2] Shepherd, D., McBride, D., Welch, D., Dirks, K. N., and Hill, E. M. (2011). Evaluating the impact of wind turbine noise on health-related quality of life. Noise and Health, Vol. 13, No. 54, pp. 333.

[3] Nissenbaum, M.A., Aramini, J. J., and Hanning, C.D. (2012). Effects of industrial wind turbine noise on sleep and health. Noise and Health, Vol. 14, No 60, pp. 237.

[4] Bakker, R.H., Pedersen, E., van den Berg, G.P., Stewart, R.E., Lok, W., and Bouma, J. (2012). Impact of wind turbine sound on annoyance, self-reported sleep disturbance and psychological distress. Science of the Total Environment, Vol. 425, pp. 42-51.

[5] Van Renterghem, T., Bockstael, A., De Weirt, V., and Botteldooren, D. (2013). Annoyance, detection and recognition of wind turbine noise. Science of the Total Environment, Vol. 456, pp. 333-345.

[6] Inagaki, T., Li, Y., and Nishi, Y. (2015). Analysis of aerodynamic sound noise generated by a large-scaled wind turbine and its physiological evaluation. International Journal of Environmental Science and Technology, Vol 12, No. 6, pp.1933-1944.

[7] Swinbanks, M. (2015). Direct experience of low frequency noise and infrasound within a windfarm community. 6th International Meeting on Wind Turbine Noise, Glasgow, USA.

[8] Luo, K., Zhang, S., Gao, Z., Wang, J., Zhang, L., Yuan, R., Fan, J., and Cen, K. (2015). Large-eddy simulation and wind-tunnel measurement of aerodynamics and aeroacoustics of a horizontal-axis wind turbine. Renewable Energy, Vol. 77, pp. 351-362.

[9] Maizi, M., Mohamed, M.H., Dizene, R., and Mihoubi, M. C. (2018). Noise reduction of a horizontal wind turbine using different blade shapes. Renewable Energy, Vol. 117, pp. 242-256.

[10] Zhang, Sanxia, Kun Luo, Renyu Yuan, Qiang Wang, Jianwen Wang, Liru Zhang, and Jianren Fan. (2018). Influences of operating parameters on the aerodynamics and aeroacoustics of a horizontal-axis wind turbine. Energy, Vol. 160, pp. 597-611.

[11] Williams, J.F. and Hawkings, D.L. (1969). Sound generation by turbulence and surfaces in arbitrary motion. Philosophical Transactions for the Royal Society of London. Series A, Mathematical and Physical Sciences, pp. 321-342.

[12] Bozorgi, A., Ghorbaniasl, G., and Nourbakhsh, S.A. (2019). The reduction in low-frequency noise of horizontal-axis wind turbines by adjusting blade cone angle. International Journal of Environmental Science and Technology, Vol 16, No. 6, pp. 2573-2586.

[13] Hand, M.M., Simms, D.A., Fingersh, L.J., Jager, D.W., Cotrell, J.R., Schreck, S., and Larwood, S.M. (2001). Unsteady aerodynamics experiment phase VI: wind tunnel test configurations and available data campaigns (No. NREL/TP-500-29955). National Renewable Energy Lab., Golden, CO.(US).

[14] Wagner, S., Bareiss, R., and Guidati, G. (1996). Wind Turbine Noise. New York, Springer.

[15] Bozorgi, A. and Ghorbaniasl, G. (2020). Determination of significant sources generating low-frequency noise in horizontal axis wind turbines. Energy Equipment and Systems, Vol. 8, No. 3, pp. 253-262.

[16] Ghorbaniasl, G. and Lacor, C. (2012). A moving medium formulation for prediction of propeller noise at incidence. Journal of Sound and Vibration, Vol. 331, No. 1, pp. 117-137.